Diffusion and vibration of CO molecules adsorbed on a Cu(100) surface: A periodic density functional theory study

Fouquet, P.; Olsen, R.A.; Baerends, E.J.

published in
Journal of Chemical Physics
2003

DOI (link to publisher)
10.1063/1.1578054

document version
Publisher's PDF, also known as Version of record

Diffusion and vibration of CO molecules adsorbed on a Cu(100) surface: A periodic density functional theory study

Peter Fouquet[a)]
Cavendish Laboratory, University of Cambridge, Madingley Road, Cambridge CB3 0HE, United Kingdom

Roar A. Olsen and Evert Jan Baerends
Department of Theoretical Chemistry, Vrije Universiteit, De Boelelaan 1083, 1081 HV Amsterdam, The Netherlands

(Received 21 October 2002; accepted 7 April 2003)

The potential energy surface (PES) describing the diffusion and vibration of CO molecules adsorbed on a Cu(100) surface has been calculated using density functional theory within two different generalized gradient approximations (GGAs), employing a slab representation of the surface. One goal of the study was to investigate the origin of the discrepancy between a recently published PES [J. Chem. Phys. **114**, 1053 (2001)] and inferences that had been made from various experiments. A further aim was to create a PES that could provide a better basis for modeling and understanding of the diffusive and vibrational motion in the CO/Cu(100) system. We found that the calculated PES has a global minimum on-top of the substrate atoms in line with the experimentally determined adsorption site. Diffusion is preferred across the bridge site, a saddle point, with a diffusion barrier of 95 ± 30 meV and 125 ± 30 meV for the two GGAs. Vibrational frequencies deduced from the PES agree with experimental results to within 10 meV. © *2003 American Institute of Physics.*
[DOI: 10.1063/1.1578054]

I. INTRODUCTION

The potential energy surface (PES) describing the lateral motion of atoms or molecules on a surface is crucial for the understanding of a wide range of phenomena spanning, e.g., surface diffusion, sliding friction, catalysis, and phase transitions in two dimensional layers. The development of reliable PESs, however, has been difficult because of the small energy differences that have to be treated accurately. CO adsorbed on Cu(100) has developed into a ''benchmark'' system because of its relative electronic simplicity and its good experimental approachability. Experimentally, the CO/Cu(100) PES is well characterized in the vicinity of the most stable adsorption site for the CO molecule. A wide range of techniques has provided information about the adsorption geometry,[1–3] the vibrational frequencies,[4–6] and the binding energy.[7] The experiments indicate that the preferred adsorption site is on-top of the substrate atoms,[3] and a number of theoretical studies agree with this result.[8–12]

However, for geometries other than in the vicinity of the most stable adsorption site there is little and contradictory information. At present only two techniques are available for reasonably accurate studies of a larger part of the PES: A theoretical approach based on periodic density functional theory (DFT) calculations and an experimental approach employing quasielastic helium atom scattering (QHAS). It is believed that the diffusion path follows a top-bridge-top line, but theoretical and experimental studies disagree on the barrier height and the shape of the PES in the vicinity of the bridge site.[13–15] A recent plane-wave based periodic DFT study employing a pseudopotential approximation found a sharp potential minimum at the bridge site in addition to a local minimum at the top site.[15] QHAS experiments, on the other hand, assume a smooth potential with a global minimum at the top site and no further local minima.[13] Because of limited QHAS energy resolution it is, however, not possible at present to make a conclusive experimental decision on the existence of local minima on the CO/Cu(100) PES.[16] New developments in QHAS, i.e., replacement of the time-of-flight method by spin-echo,[16–18] make it seem possible that this information will be available in the near future.

One of our goals in this study is to investigate how well the different DFT approximations perform when compared to the known experimental results, and at the same time possibly provide a basis for a better modeling and understanding of future experiments on the diffusive and vibrational motion of CO molecules adsorbed on a Cu(100) surface. Another goal is to see if a different computational DFT approach will support the results presented in Ref. 15, or maybe bring the theoretical results more in line with the experimental expectations.

This paper is organized as follows: In the following section the calculational details are outlined. The results of our calculations and a comparison with earlier studies are presented in Sec. III, which is followed by our conclusions in Sec. IV.

II. CALCULATIONAL DETAILS

We have used ADF-BAND[19–21] to solve the Kohn–Sham equations[22,23] self-consistently for a CO molecule adsorbed on a Cu(100) surface, which is modeled by a slab with translational symmetry in two directions. A flexible ba-

[a)]Electronic mail: pf231@cam.ac.uk

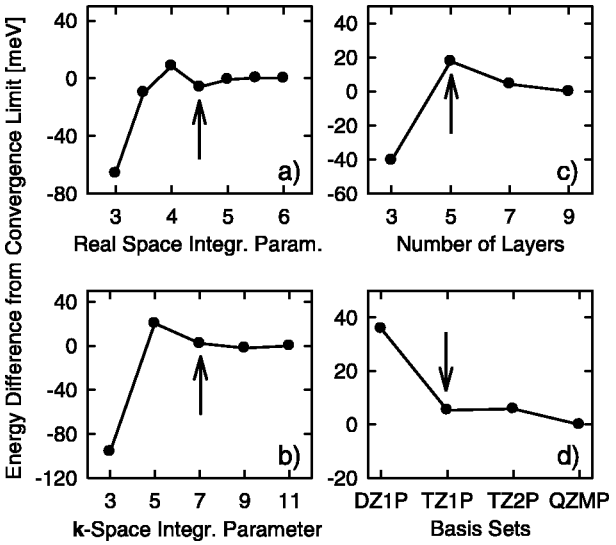

FIG. 1. Calculations testing the convergence of the diffusion barrier: (a) convergence with increasing real space integration parameter; (b) convergence with increasing **k**-space integration parameter, (c) convergence with an increasing number of Cu layers; and (d) convergence with an increasing size of basis sets (for the denomination of basis sets refer to Table I). All results are calculated for a CO molecule adsorbed in a $c(2\times2)$ structure on one side of the Cu(100) slab calculated within the BP approximation. Parameters used in the geometrical relaxation calculations (Sec. III A) are indicated by arrows.

sis set consisting of a combination of numerical atomic orbitals obtained from numerical Herman–Skillman-type calculations[24] and Slater-type orbitals has been used in the expansion of the one-electron states. It is worth noting that full convergence with respect to the basis set can be obtained without the use of plane waves, as has been demonstrated in

TABLE I. The basis sets used in the CO/Cu(100) calculations. An NAO is a numerical atomic orbital, and the numbers refer to the exponents (in units of a_0^{-1}) of a Slater-type orbital. Orbitals not indicated were kept frozen.

Element	basis label	basis
Cu	QZMP	3*s*(NAO,7.65,3.7), 3*p*(NAO,6.95,3.05), 3*d*(NAO,11.1,6.25,3.4,0.97), 4*s*(NAO,2.8,1.8,0.79), 4*p*(2.0,1.0),4*f*(4.0,2.0,1.0)
	TZ2P	3*s*(NAO,6.6), 3*p*(NAO,6.95,3.05), 3*d*(NAO,6.9,1.28), 4*s*(NAO,2.45,0.85), 4*p*(1.37), 4*f*(2.2)
	TZ1P	3*s*(NAO,6.6), 3*p*(NAO,6.95,3.05), 3*d*(NAO,6.9,1.28), 4*s*(NAO,2.45,0.85), 4*p*(1.37)
	DZ1P	3*s*(NAO,6.45), 3*p*(NAO,6.0), 3*d*(NAO,6.9,1.28), 4*s*(NAO,1.0), 4*p*(1.37)
O	QZMP	2*s*(NAO,7.1,3.2,1.5,0.75),2*p*(NAO,5.7,3.05,1.0), 3*d*(2.5,1.5), 4*f*(4.0,2.0)
	TZ2P	2*s*(NAO,7.58,2.88),2*p*(NAO,4.08,1.12),3*d*(2.0), 4*f*(3.0)
	TZ1P	2*s*(NAO,7.58,2.88), 2*p*(NAO,4.08,1.12), 3*d*(2.0)
	DZ1P	2*s*(NAO,2.82), 2*p*(NAO,3.06), 3*d*(2.0)
C	QZMP	2*s*(NAO,5.9,2.55,1.16),2*p*(NAO,5.15,2.4,0.78), 3*d*(2.5,1.5), 4*f*(4.0,2.0)
	TZ2P	2*s*(NAO,4.6,2.1), 2*p*(NAO,2.94,0.82), 3*d*(2.2), 4*f*(3.3)
	TZ1P	2*s*(NAO,4.6,2.1), 2*p*(NAO,2.94,0.82), 3*d*(2.2)
	DZ1P	2*s*(NAO,1.98), 2*p*(NAO,2.2), 3*d*(2.2)

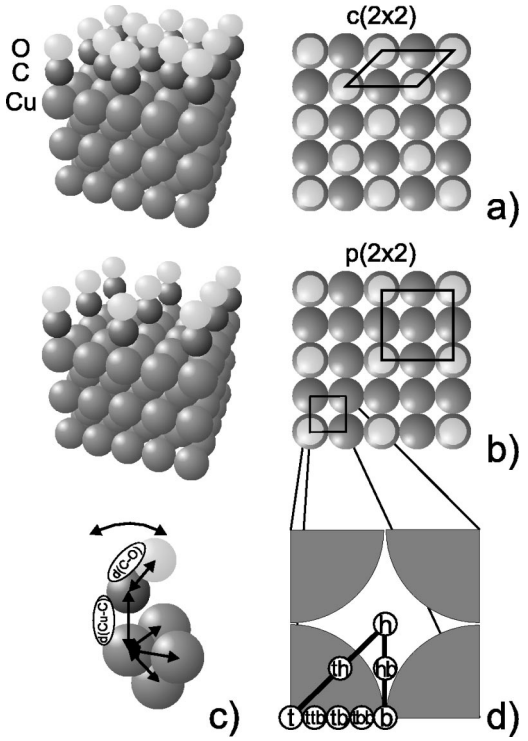

FIG. 2. Geometries used in this study. (a), (b) Geometries of the $c(2\times2)$ and $p(2\times2)$ CO superstructures, respectively, on the five layer Cu slabs. On the top views the surface unit cells are indicated. (c) The distances and angles optimized during relaxation. (d) Points of the unit cell for which adsorption energies have been calculated in this study.

the past.[20] The calculations can in princple be performed with all electrons included in the variational space. However, deeper lying electronic levels are kept frozen when explicit tests show that their variational inclusion has a negligible effect. Pseudopotentials are never used. The calculation of the matrix elements of the Hamiltonian is performed by product Gauss numerical integration rules within the pyramids that constitute the Voronoi polyhedra surrounding the atoms.[21] (The Voronoi polyhedron of an atom is the part of space that is closer to that atom than to any other one; in regular crystals these become the Wigner–Seitz cells.) A single parameter (the real space integration parameter) governs the precision of the numerical integration; a value q corresponds to relative precision 10^{-q} in the integrals. Finally, the **k**-space integration can be done very accurately using the quadratic tetrahedron method.[25]

The exchange-correlation energy in the local density approximation (LDA) is calculated using the Vosko–Wilk–Nusair formulas.[26] Two generalized gradient approximations (GGAs) are employed in this study. The first combines the Becke correction[27] for the exchange energy with the Perdew correction[28] for the correlation energy (BP), and the second is the gradient-corrected functional of Perdew *et al.*[29,30] (PW GGA-II, which we will label PW for brevity). All results are given including scalar relativistic corrections through the zeroth-order regular approximation[31–33] unless explicitly stated otherwise.

Recent work on the CO/Cu(100) PES suggests the diffusion barrier to be between 40 and 80 meV.[13–15] For our calculations to be able to test the quality of the different

TABLE II. Equilibrium distances for CO molecules with the molecular axis normal to the Cu(100) surface plane at different surface sites [shown in Fig. 2(d)]. The C–Cu distance is denoted d(C–Cu) and measures the height of the C atom above the surface plane [see Fig. 2(c)]. The distance between the C and the O atom in the CO molecule is denoted d(C–O). The results are for a $c(2\times2)$ structure employing the BP approximation. All distances are in Å.

	t	ttb	tb	tbb	b	hb	h	th
d(C–Cu)	1.86	1.83	1.78	1.66	1.57	1.47	1.30	1.68
d(C–O)	1.15	1.15	1.16	1.16	1.16	1.17	1.18	1.16

density functional theory (DFT) approximations for this system, and possibly contribute to the increased understanding of the diffusive motion of CO on Cu(100), the accuracy of the calculations should approach 10–20 meV for relative energies (e.g., the diffusion barrier). Figure 1 shows that the chosen computational parameters are sufficient to reach this goal: (a) A real space integration accuracy better than 10 meV in the chemisorption energy is reached by setting the real space integration parameter to 4.5. (b) Setting of the **k**-space integration parameter to 7 results in an error below 10 meV. [A **k**-space integration parameter of 7 corresponds to 28 points in the irreducible wedge of the surface Brillouin zone in the highest symmetry cases (e.g., CO perpendicular to the surface above a top site), and 43 points in the lower symmetry cases (e.g., CO not perpendicular to the surface above a bridge site). Note that these numbers of **k**-points are not directly comparable to the numbers in lower order **k**-space integration methods such as the linear tetrahedron method[34] or Monkhorst–Pack method,[35] due to the more rapid convergence of the quadratic tetrahedron method.] (c) A five layer slab gives results that differ by about 20 meV from a nine layer slab. (d) The TZ1P basis set (triple zeta, i.e., three basis functions per valence orbital, plus one polarization function) gives results that are within 10 meV of the results based on the TZ2P (triple zeta plus two polarization functions) and QZMP (quadruple zeta, i.e., four or more basis functions per valence orbital plus four or more polarization functions) basis sets. The QZMP basis set is very large, with a proven accuracy of bond energies at the 10 meV level.[36] The different basis sets tested are shown in Table I. (e) All results remain unchanged upon unfreezing the $1s$ orbital of C and O, and the $1s$, $2s$, and $2p$ orbitals of Cu (not shown in Fig. 1).

Computational aspects concerning the choice of the Cu–Cu distance in the slab, the size of the surface unit cell, the effect of neglecting relativistic corrections, and the way the CO adsorption geometries have been found are discussed in Sec. III.

TABLE III. Tilting angles for CO molecules adsorbed at the eight different surface sites shown in Fig. 2(d), with the d(C–Cu) and d(C–O) distances as given in Table II. The tilting directions were chosen to be along the lines of highest symmetry, e.g., in the direction towards the bridge site for the ttb, tb, and tbb sites. The results were calculated for the BP approximation.

t	ttb	tb	tbb	b	hb	h	th
0°	8.46°	13.93°	12.05°	0°	9.59°	0°	17.04°

TABLE IV. A comparison between available results for the equilibrium distances for CO molecules with the molecular axis normal to the Cu(100) surface plane at three surface sites and in the gas phase (all distances are in Å).

	This study	Ref. 9	Ref. 10	Ref. 12	Experiment
d(C–Cu) top	1.86	1.94	1.85	1.88	1.90[a] 1.92[b]
d(C–O) top	1.15	1.15	1.14	1.16	1.15[a] 1.13[b]
d(C–Cu) bridge	1.57	1.63		1.56	
d(C–O) bridge	1.16	1.15		1.16	
d(C–Cu) hollow	1.30	1.34		1.21	
d(C–O) hollow	1.18	1.17		1.16	
d(C–O) gas phase	1.15		1.12	1.15	1.13[c]

[a]Reference 2.
[b]Reference 3.
[c]Reference 37.

III. RESULTS AND DISCUSSION

A. Adsorption geometries

The CO molecule has been adsorbed within a $c(2\times2)$ structure on the eight different surface sites shown in Fig. 2. For each site the equilibrium position in d(C–Cu) (the distance of the C atom above the Cu surface plane) and d(C–O) (the distance between the C and the O atom) have been found through a two-dimensional cubic spline interpolation based on 25 or more calculated points for CO molecules adsorbed with the molecular axis normal to the Cu(100) surface plane. The results for the BP approximation are given in Table II. For each of the resulting equilibrium geometries nine calculations have been performed with the CO molecular axis forming different angles with the surface normal (the position of the C atom is being kept fixed; see Fig. 2). Each of these data sets have been interpolated with a third order polynomial, and the optimal angles found are given in Table III. The tilting directions were chosen to be along the lines of highest symmetry, i.e., in the top-bridge direction for the ''ttb,'' ''tb,'' and ''tbb'' sites, in the top-hollow direction for ''th'' site, and in the hollow-bridge direction for the ''hb'' site. The CO molecules were found to be tilted following the shape of the effective corrugation of the surface charge density, i.e., bent towards the bridge site for the ''ttb,'' ''tb,'' and ''tbb'' sites and bent towards the hollow site for the ''th'' and ''hb'' sites. This finding is in line with a recent cluster PES calculation by Bagus and Wöll.[11]

As seen from Table IV a comparison of the equilibrium geometries found in this study to those found in other theoretical studies, and also to the results of experiments, show a rather good mutual agreement. This indicates that the challenges when seeking to obtain a reliable PES for the CO/Cu(100) system will be found in the other aspects of the theoretical calculations or the experiments.

B. Diffusion barrier

Based on the results in Sec. III A a cubic spline fitted two-dimensional PES for CO motion along the surface is shown in Fig. 3. A view of the potential along the most probable diffusion path (a ⟨110⟩ direction) is given in Fig. 4.

The following additional tests have been performed to ensure proper convergence of the results: (i) For the equilib-

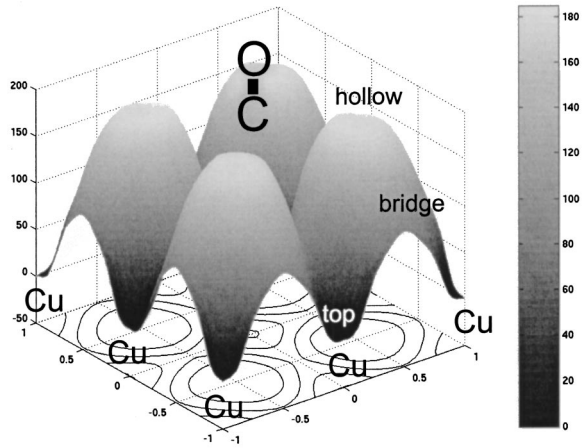

FIG. 3. Adiabatic lateral potential energy surface for CO molecules on the Cu(100) surface based on a $c(2\times2)$ structure. The relative adsorption energies are given in meV.

rium geometries the calculations have been repeated with CO adsorbed in a $p(2\times2)$ structure. The diffusion barrier decreases by about 20 meV when lowering the coverage from 50% to 25%. (ii) All results reported above have been obtained for CO adsorbed on a Cu slab with the Cu–Cu distance being the experimental bulk lattice constant (4.83 bohr). Using a theoretical bulk optimized lattice constant decreases the barrier by less than 10 meV. (iii) A relaxation of the top Cu layer has been performed giving rise to an increase in the barrier height that is smaller than 15 meV. (iv) As expected for the CO/Cu(100) system, relativistic effects are not very important. Performing the calculations nonrelativistically changes the diffusion barrier by less than 5 meV

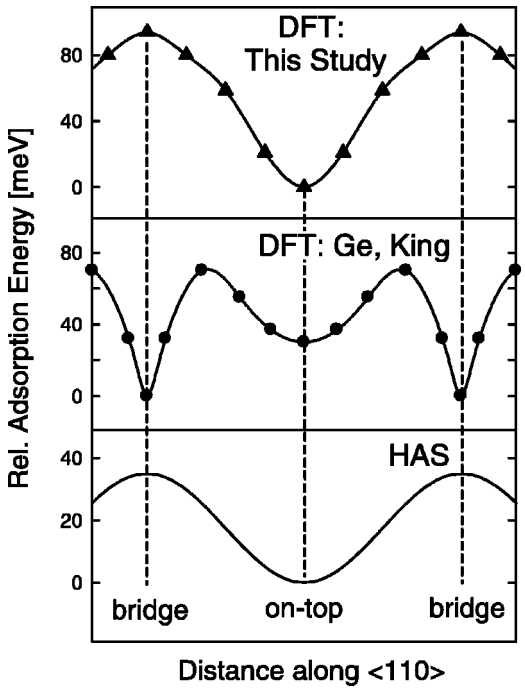

FIG. 4. Cut through the CO/Cu PES along the ⟨110⟩ direction. (a) Data of this study; (b) DFT PES by Ge and King (Ref. 15); and (c) helium atom scattering data by Graham *et al.* (Refs. 13 and 14).

TABLE V. The calculated diffusion barrier in meV for the GGA approximations. All corrections described in Sec. III B (bulk relaxation, etc.) were included.

	BP	PW
$c(2\times2)$	115 ± 30	145 ± 30
$p(2\times2)$	95 ± 30	125 ± 30

as compared to calculations including scalar relativistic corrections.

The only remaining test to perform is to check the influence of changing the DFT functional. All the calculations above have been performed self-consistently on the LDA level, applying the GGA correction to the self-consistent LDA electron density. Performing the calculations fully self-consistently on the GGA level introduces an increase in the BP diffusion barrier height of less than 20 meV. For the PW diffusion barrier the effect is larger as the barrier increases by about 50 meV. The extensive tests performed here and in Sec. II make us believe that we have converged the result for the diffusion barrier to within ±30 meV of the DFT GGA limits for the CO/Cu(100) system. The barrier obtained by the different DFT approximations are given in Table V. The PW functional appears to give a 30 meV higher barrier than the BP functional.

For the CO/Pt(111) system it has been proposed that DFT within the most commonly used GGA approximations does not find the correct adsorption site, the top site, but prefers the hollow site, and, therefore, does not describe the shape of the PES reliably.[38] We have, however, recently found in extensive tests on that particular system[39] that when the computational precision is pushed sufficiently high, there is in fact a small energetic preference for the top site above the bridge site within the GGAs of DFT, of the right order of magnitude (about 60 meV). Also for the CO/Cu(100) system there does not seem to be an anomaly. The results in Sec. III A indicate that DFT at the GGA level finds the correct adsorption site, and the results of this section suggest that the agreement for the shape of the PES between our calculations and experiments is rather good (see Fig. 4). This view is also supported by the results of the next section. It is to be noted that a lower value is found experimentally for the activation energy E_{act} for diffusion in QHAS experiments (31 meV) compared to the barrier on the adiabatic PES [95 ± 30 meV for $p(2\times2)$ with the BP functional]. But we do wish to note that our calculated adiabatic barrier heights cannot be compared directly to the QHAS activation energy of 31 meV. It is necessary to perform extensive MD simulations on the adiabatic PES, including frictional coupling of the adsorbate motion to the surface, to deduce the equivalent of the QHAS measured activation energy from the PES. Such simulations always lead to considerably lower E_{act} than the PES barrier height.[16] This is true for the CO/Cu(001) surface of Ge and King,[15] where the PES barrier of 70 meV reduces to a simulated QHAS E_{act} of about 40 meV. Jardine *et al.*[16] observed such a reduction also with other PESs, such as that for Na/Cu(001) and an earlier trial PES for CO/Cu(001), and noted that a simple Arrhenius type of analysis of the QHAS data

TABLE VI. A comparison of theoretical and experimental vibrational frequencies for $c(2\times2)$-CO/Cu(100), in meV.

Mode	This study	Ref. 8	Ref. 10	Ref. 11	Ref. 12	Ref. 40	Ref. 41	Ref. 42	Ref. 43	Experiment
T	6	0.5	1.61	4.56		12.6		3.84	3.39	3.93(2)[a]
R	26	44.3	34.96	35.43		26.5		43.8	41.3	35.61(2)[a]
S	46	46.1	52.9	21.48	46.8	49.4	25.5	43.3	43.1	42.72(2)[a]
C–O str.	250	270.1	261.9		251.2	248.9	266.7	264.3	267.0	258.6[b]

[a]Reference 6.
[b]Reference 44.

underestimates the adiabatic barrier by a significant and unknown margin. We therefore expect MD simulations to remove at least part of the discrepancy between our calculated barrier height and the lower QHAS E_{act}, but it appears likely that the adiabatic DFT GGA barrier will still prove to be somewhat too high.

As can be seen in Fig. 4 the agreement between our results and the results of a recent plane-wave based periodic DFT study employing a pseudopotential approximation is not very good for the shape of the PES. Whether this discrepancy is a result of the pseudopotential approximation employed in Ref. 15 or an insufficient convergence in other computational parameters should be addressed in the future.

C. Vibrational frequencies

In addition to the lateral adiabatic PES, which is described above, the geometrical relaxation calculations provide the basis for a vibrational analysis. The frequency ω of mode α can be calculated from the curvature of the full PES $V(\mathbf{x})$ via $\hbar\omega_\alpha=\sqrt{(1/m)\,d^2V(\mathbf{x}_\alpha)/d\mathbf{x}_\alpha^2}$, where m is the effective mass of the vibrating particle. Normal mode analysis results in four normal modes attributed to the CO molecules: (i) a frustrated translational mode (commonly denoted *T*), (ii) a frustrated rotational mode (denoted *R*), (iii) a vibration of the entire molecule against the copper substrate (denoted *S*), and (iv) the internal vibrational mode of the CO molecule. The values derived from the present PES are listed in Table VI, which also contains other theoretical and experimental literature data. The comparison with this data provides an additional accuracy check of the present calculations in the vicinity of the adsorption site. The benchmark has to be the experimental data in this case, because of its high energy resolution.[6,44] The vibrational frequencies derived from the present PES have a deviation from experimental data of less than 10 meV. This is well in line with the general accuracy aimed for.

We would like to note that in Sec. III B we estimated the computational error bar for the barrier height to be ±30 meV. In the light of this computational limitation, we cannot expect anything but qualitative agreement between the *T*, *R*, and *S* mode frequencies calculated with our PES and experiment. But that is indeed what is obtained (see Table VI). We feel that these frequencies substantiate that our PES is basically sound. We are content that we do find the *T* mode frequency to be quite low, but it is not clear if we can attach any significance to the difference between calculation (6 meV) and experiment (4 meV). To do this in a meaningful way, the numerical precision of the calculations would have to be pushed much higher than it is now.

IV. CONCLUSIONS

Through density functional theory (DFT) employing two different generalized gradient approximations (GGAs) we have calculated the potential energy surface (PES) describing the diffusion and vibration of CO molecules adsorbed on a Cu(100) surface, using a slab representation of the surface. Since the relevant energy differences are in the 10–100 meV range a considerable effort was made to reduce the calculational error. A careful testing of all computational parameters indicates that we have been able to converge our results to within ±30 meV of the DFT GGA limits for the CO/Cu(100) system.

We found that the calculated PES has a global minimum on-top of the substrate atoms in line with the experimentally determined adsorption site. As suggested by experiments we found that the diffusion preferentially follows a top-bridge-top line, with a calculated diffusion barrier of 95 ± 30 meV and 125 ± 30 meV for the two GGAs. All calculated vibrational frequencies agree with experimental results within 10 meV. We note that the present PES does not exhibit the deep well at the bridge site, which was a conspicuous feature of an earlier DFT GGA PES by Ge and King.[15] This part of the potential seemed to be at variance with the deductions made from low energy electron diffraction (LEED),[2] x-ray absorption and photelectron diffraction measurements,[3] and quasi-elastic helium atom scattering (QHAS) data.[14] It is gratifying that our calculated PES does not exhibit anomalous features compared to experiment. It is possible that the pseudopotential approximation of the pseudopotential plane wave method employed by Ge and King is not reliable at the very high level of accuracy that is needed here. The Cu pseudopotential may have a slightly different effect for adsorption at on-top and bridge sites.

Our results indicate that the two GGAs tested compare favorably to the known experimental data, and this suggests that the DFT GGA approach used here might be very helpful for providing a basis for a better modeling and understanding of the diffusive and vibrational motion in the CO/Cu(100) system.

ACKNOWLEDGMENTS

The authors would like to thank Dr. W. Allison, Dr. J. Ellis, and Dr. A. P. Jardine for interesting and helpful discussions. P.F. is grateful for the support by a European Community Marie Curie Fellowship. The research of R.A.O. was financed by the Dutch National Research Council–Chemical Sciences (NWO–CW) and the National Research School Combination ''Catalysis Controlled by Chemical Design'' (NRSC-Catalysis).

[1] J. C. Tracy, J. Chem. Phys. **56**, 2748 (1972).
[2] S. Andersson and J. B. Pendry, Phys. Rev. Lett. **43**, 363 (1979).
[3] C. F. McConville, D. P. Woodruff, K. C. Prince, G. Paolucci, V. Chab, M. Surman, and A. M. Bradshaw, Surf. Sci. **166**, 221 (1986).
[4] C. J. Hirschmugl, G. P. Williams, F. M. Hoffmann, and Y. J. Chabal, Phys. Rev. Lett. **65**, 480 (1990).
[5] J. Ellis, G. Witte, and J. P. Toennies, J. Chem. Phys. **102**, 5059 (1995).
[6] A. P. Graham, F. Hofmann, J. P. Toennies, G. P. William, C. Hirschmugl, and J. Ellis, J. Chem. Phys. **108**, 7825 (1998).
[7] C. M. Truong, J. A. Rodriguez, and D. W. Goodman, Surf. Sci. Lett. **271**, L385 (1992).
[8] J. C. Tully, M. Gomez, and M. Head-Gordon, J. Vac. Sci. Technol. A **11**, 1914 (1993).
[9] P. H. T. Philipsen, G. te Velde, and E. J. Baerends, Chem. Phys. Lett. **226**, 583 (1994).
[10] S. P. Lewis and A. M. Rappe, Phys. Rev. Lett. **77**, 5241 (1996).
[11] P. S. Bagus and C. Wöll, Chem. Phys. Lett. **294**, 599 (1998).
[12] F. Favot, A. Dal Corso, and A. Baldereschi, J. Chem. Phys. **114**, 483 (2001).
[13] A. P. Graham and J. P. Toennies, Surf. Sci. **427/428**, 1 (1999).
[14] A. P. Graham and J. P. Toennies, J. Chem. Phys. **114**, 1051 (2001).
[15] Q. Ge and D. A. King, J. Chem. Phys. **111**, 9461 (1999); **114**, 1053 (2001).
[16] A. P. Jardine, J. Ellis, and W. Allison, J. Phys.: Condens. Matter **14**, 6173 (2002).
[17] M. DeKieviet, D. Dubbers, C. Schmidt, D. Scholz, and H. Spinola, Phys. Rev. Lett. **75**, 1919 (1995).
[18] A. P. Jardine, P. Fouquet, J. Ellis, and W. Allison, Rev. Sci. Instrum. **72**, 3834 (2001).
[19] G. te Velde, Ph.D. thesis, Vrije Universiteit, Amsterdam, 1990.
[20] G. te Velde and E. J. Baerends, Phys. Rev. B **44**, 7888 (1991).
[21] G. te Velde and E. J. Baerends, J. Comput. Phys. **99**, 84 (1992).
[22] P. Hohenberg and W. Kohn, Phys. Rev. **136**, B864 (1964).
[23] W. Kohn and L. J. Sham, Phys. Rev. **140**, A1133 (1965).
[24] F. Herman and S. Skillman, *Atomic Structure Calculations* (Prentice-Hall, Englewood Cliffs, NJ, 1963).
[25] G. Wiesenekker, G. te Velde, and E. J. Baerends, J. Phys. C **21**, 4263 (1988).
[26] S. H. Vosko, L. Wilk, and M. Nusair, Can. J. Phys. **58**, 1200 (1980).
[27] A. D. Becke, Phys. Rev. A **38**, 3098 (1988).
[28] J. P. Perdew, Phys. Rev. B **33**, 8822 (1986).
[29] J. P. Perdew, in *Electronic Structure of Solids '91*, edited by P. Ziesche and H. Eschrig (Akademie-Verlag, Berlin, 1991).
[30] J. P. Perdew, J. A. Chevary, S. H. Vosko, K. A. Jackson, M. R. Pederson, D. J. Singh, and C. Fiolhais, Phys. Rev. B **46**, 6671 (1992).
[31] E. van Lenthe, Ph.D. thesis, Vrije Universiteit, Amsterdam, 1996.
[32] E. van Lenthe, E. J. Baerends, and J. G. Snijders, J. Chem. Phys. **101**, 9783 (1994).
[33] P. H. T. Philipsen, E. van Lenthe, J. G. Snijders, and E. J. Baerends, Phys. Rev. B **56**, 13556 (1997).
[34] G. Lehmann and M. Taut, Phys. Status Solidi B **54**, 469 (1972).
[35] H. J. Monkhorst and J. D. Pack, Phys. Rev. B **13**, 5188 (1976).
[36] E. van Lenthe and E. J. Baerends, J. Comput. Chem. (to be published).
[37] K. P. Huber and G. Herzberg, in *Molecular Spectra and Molecular Structure, IV. Constants of Diatomic Molecules* (Van Nostrand Reinhold, New York, 1979), p. 166.
[38] P. J. Feibelmann, B. Hammer, J. K. Nørskov, F. Wagner, M. Scheffler, R. Stumpf, R. Watwe, and J. Dumesic, J. Phys. Chem. B **105**, 4019 (2001).
[39] R. A. Olsen and E. J. Baerends, J. Chem. Phys. (to be published).
[40] M. A. van Daelen, Y. S. Li, J. M. Newsam, and R. A. van Santen, J. Phys. Chem. **100**, 2279 (1996).
[41] J. Casanovas and G. Pacchioni, Chem. Phys. Lett. **259**, 438 (1996).
[42] S. C. Park, W. K. Park, and J. M. Bowman, Surf. Sci. **427/428**, 343 (1999).
[43] A. Bahel and Z. Bačić, J. Chem. Phys. **111**, 11164 (1999).
[44] R. Ryberg, Surf. Sci. **114**, 627 (1982).